Arteriosclerosis, Thrombosis, and Vascular Biology
JOURNAL OF THE AMERICAN HEART ASSOCIATION

Human LDL Receptor Enhances Sequestration of ApoE4 and VLDL Remnants on the Surface of Hepatocytes but Not Their Internalization in Mice

Michael Altenburg, Jose Arbones-Mainar, Lance Johnson, Jennifer Wilder and Nobuyo Maeda

Arterioscler Thromb Vasc Biol 2008, 28:1104-1110: originally published online March 27, 2008
doi: 10.1161/ATVBAHA.108.164863
Arteriosclerosis, Thrombosis, and Vascular Biology is published by the American Heart Association.
7272 Greenville Avenue, Dallas, TX 72514
 Print ISSN: 1079-5642. Online ISSN: 1524-4636

Human LDL Receptor Enhances Sequestration of ApoE4 and VLDL Remnants on the Surface of Hepatocytes but Not Their Internalization in Mice

Michael Altenburg, Jose Arbones-Mainar, Lance Johnson, Jennifer Wilder, Nobuyo Maeda

Objective—In humans, apolipoprotein (apo) E4 is associated with elevated plasma cholesterol levels and a high risk of developing atherosclerosis, whereas apoE2 is protective. Here we investigate the mechanism by which mice expressing human apoE isoforms recapitulate this association when they also express high levels of human low-density lipoprotein receptor (LDLR).

Methods and Results—Primary hepatocytes from apoE4 mice secreted less apoE into the medium than hepatocytes from apoE2 mice. Increased LDLR expression decreased this secretion and increased degradation of apoE4. An apoE4-GFP fusion protein expressed in the liver of apoE-deficient mice accumulated on the hepatocyte surface bordering the space of Disse in an LDLR-dependent manner. Fluorescence-labeled very low–density lipoprotein (VLDL) remnants accumulated on the hepatocyte surface in apoE4 mice with high LDLR, but they were internalized poorly. In contrast, apoE2-GFP did not accumulate on the hepatocyte surface even when the LDLR expression was high, but apoE2 mice with high LDLR internalized the remnants avidly without sequestering them on the hepatocyte surface.

Conclusions—The high affinity of apoE4 to the LDLR enhances VLDL sequestration on the hepatocyte surface but delays their internalization. This delay likely increases VLDL conversion to cholesterol-enriched remnants in apoE4 mice with high LDLR, and probably to LDL in humans with apoE4. (***Arterioscler Thromb Vasc Biol*. 2008;28:1104-1110**)

Key Words: mouse models ■ lipoprotein metabolism ■ space of Disse ■ recombinant adenovirus

Apolipoprotein E (apoE) and the low-density lipoprotein receptor (LDLR) play a pivotal role in the clearance of lipoproteins by the liver, thereby reducing plasma cholesterol, a leading determinant of atherosclerosis susceptibility.[1,2] Uptake of triglyceride-rich lipoproteins (TRL) occurs via multiple receptors and perhaps in several steps.[3] The first, most important step appears to be the sequestration of TRL on the microvilli of hepatocytes, where LDLR, heparan sulfate proteoglycans (HSPG), and LDLR related proteins (LRP) are located. These molecules bind apoE proteins secreted by the liver thereby serving as reservoirs for enriching remnant particles with apoE.[4] They also serve as the receptors for internalization of apoE-enriched remnants.[3]

In humans, the *Apoe* gene is polymorphic, resulting in production of 3 common isoforms, apoE2, E3, and E4. They differ in primary structure at 2 positions, E2 having Cys at both positions 112 and 158, E3 having a Cys at 112 and an Arg at 158, and E4 having Arg at both positions. They also differ in their LDLR binding affinity; apoE4 binds LDLR with a slightly higher affinity than apoE3, whereas apoE2 has much reduced binding compared to the other 2 isoforms.[5–9] Despite the low receptor binding of apoE2, the majority of individuals carrying apoE2 have lower plasma LDL cholesterol and reduced atherosclerosis risk, although 5% to 10% of apoE2 homozygotes develop type III hyperlipoproteinemia characterized by markedly elevated plasma lipid levels.[2,10] Equally paradoxical is the association of the apoE4 isoform with high LDL-cholesterol, low plasma triglycerides (TG), and an increased risk of atherosclerosis.[1,2,10–14] How the different apoE isoforms lead to different plasma lipoprotein profiles in vivo remains unclear, and mice with the wild-type *Apoe* gene replaced with human alleles do not simply replicate human phenotypes. Thus, all mice expressing apoE2 ($Apoe^{2/2}$) exhibit type III hyperlipoproteinemia and develop atherosclerosis even on a normal chow containing low cholesterol and low fat, whereas those expressing apoE3 ($Apoe^{3/3}$) or apoE4 ($Apoe^{4/4}$) are normolipidemic and do not develop atherosclerosis.[7,15,16] However, the human-like associations are replicated when the mice expressing human apoE isoforms also have 2- to 3-fold normal LDLR expression attributable to the *Ldlr*h* allele coding for human LDLR.[17–20] Both adenovirus-mediated or global overexpression of the human LDLR in mice with apoE2 results in reduction of plasma cholesterol and TG and the absence of atherosclerosis.[17,21] Mice with human apoE3 and the *Ldlr*h* allele ($Apoe^{3/3}Ldlr^{h/+}$) have significantly decreased HDL-cholesterol

Original received November 7, 2007; final version accepted March 11, 2008.

From the Department of Pathology and Laboratory Medicine, The University of North Carolina at Chapel Hill.

Correspondence to Dr Nobuyo Maeda, Department of Pathology and Laboratory Medicine, The University of North Carolina at Chapel Hill, 701 Brinkhous-Bullitt Building, Chapel Hill, NC 27599-7525. E-mail nobuyo@med.unc.edu

Arterioscler Thromb Vasc Biol is available at http://atvb.ahajournals.org DOI: 10.1161/ATVBAHA.108.164863

but only a small increase in remnants and do not develop atherosclerosis.[18] In contrast, on a high-fat Western type diet, mice with apoE4 overexpressing the LDLR (*Apoe*$^{4/4}$*Ldlr*$^{h/+}$) have increased plasma very low density lipoproteins (VLDL)/chylomicron remnants, decreased HDL-cholesterol levels, and develop atherosclerosis.[18]

The present work was aimed to test the hypothesis that the adverse effects of the increased LDLR expression in mice with apoE4 is because the higher affinity of apoE4 for the LDLR inhibits enrichment of apoE4 on apoE-poor VLDL. We show that a substantial amount of apoE4, and to a lesser extent apoE3, but not apoE2, is colocalized with LDLR on the surface of hepatocytes. This interaction with the LDLR increases the association of apoE4 with hepatocytes, limits apoE4 secretion, and enhances its degradation in primary cultured hepatocytes. It also enhances the sequestration of VLDL remnants on the hepatocyte surface, but not their internalization.

Methods

Mice

ApoE-deficient mice (*Apoe*$^{-/-}$), LDLR-deficient mice (*Ldlr*$^{-/-}$), mice homozygous for replacement of the mouse apoE gene with either the human *APOE*2*, *APOE*3*, or *APOE*4* allele (*Apoe*$^{2/2}$, *Apoe*$^{3/3}$, and *Apoe*$^{4/4}$), and mice overexpressing the human *LDLR* minigene (*Ldlr*$^{h/+}$) were individually backcrossed at least 6 generations to C57BL/6 genetic background.[7,15–17] Intercross of these mutants produced mice with various combinations of the *Apoe* and *Ldlr* loci. Mice were fed a high-fat Western-type diet (HFW) containing 21% (wt/wt) fat and 0.2% (wt/wt) cholesterol (TD88137; Teklad) for at least 2 weeks before experiments. Genotype and lipid profiles of experimental mice are presented in supplemental Table I and supplemental Figure I (available online at http://atvb.ahajournals.org). The animals were handled under protocols approved by the Institutional Animal Care and Use Committees of the University of North Carolina-Chapel Hill. For additional details on methods, please refer to the supplemental materials (available online at http://atvb.ahajournals.org).

^{35}S Labeling of Primary Mouse Hepatocytes

Primary hepatocytes were isolated as described.[22] The cells were plated onto 60-mm mouse collagen IV-coated dishes (Falcon) and pulsed with 0.5 mL medium containing ^{35}S methionine (100 μCi/mL, Amersham) for 30 or 60 minutes, and chased for 1 and 4 hours with fresh medium with excess cold methionine. ApoE was immunoprecipitated using a goat antihuman apoE antibody (Calbiochem), separated by SDS-PAGE, and visualized by a Fla-3000 phosphoimager (FujiFilm).

Adenoviruses

The plasmid vectors containing cytomegalus viral promoter-driven cDNA for fusion proteins, apoE2-GFP, apoE3-GFP, and apoE4-GFP, were provided by Dr Robert DeKroon at Duke University (Durham, NC). These vectors express fusion proteins with EGFP (enhanced green fluorescent protein) attached to the C-terminal end of each apoE isoform.[23] Adenoviral vectors encoding apoE2-GFP, apoE3-GFP, and apoE4-GFP were made using the AdEasy adenoviral system (Stratagene). Recombinant adenovirus stock, stored at −80°C, was diluted with PBS and 1×10^9 PFU in 0.2 mL of adenovirus was injected into each mouse via the tail vein.

Isolation, DiI Labeling, and Injection of VLDL

The VLDL fraction was isolated from pooled plasma by ultracentrifugation at d <1.006 g/mL and labeled with 1,1′-dioctadecyl-3,3,3′,3′- tetramethylindocarbocyanine perchlorate (DiI C_{18}; Molecular Probes Inc), as described by Stephan and Yurachek.[24] DiI-labeled VLDL (100 μg protein) was injected into tail veins of mice and livers were fixed with 4% paraformaldehyde 20 minutes later. DiI-labeled VLDL remaining in the plasma at 2 minutes, 10 minutes, and 20 minutes was determined using a microscope fluorometer (Olympus FV500 with a SPOT 2 digital camera) using a modification of the fluorometric procedure described.[25]

Microscopic Analyses

Livers were perfused through the portal vein at 2 mL/min for 2 minutes with 4% paraformaldehyde, excised from animals, and further fixed overnight in 4% paraformaldehyde. Slides with consecutive liver paraffin sections (5 μm) were used for immunohistochemistry. For confocal analysis 100-μm-thick liver sections were cut with a vibratome.

Statistical Analysis

The significance of differences between means was determined by use of 1-way ANOVA and Turkey-Kramer honestly significant difference tests (JMP software; SAS Inc).

Results

Secretion, Synthesis, and Degradation of ApoE in Primary Hepatocytes

To determine the cellular metabolism of the different apoE isoforms, we isolated primary hepatocytes from mice expressing different apoE isoforms and compared the apoE protein using Western blot analysis. After culturing in DMEM without FBS for 24 hours, primary hepatocytes from *Apoe*$^{2/2}$ mice secreted more apoE protein into the medium compared to the cells from *Apoe*$^{4/4}$ mice (Figure 1A). The ratio of medium apoE to cell-associated apoE in the *Apoe*$^{2/2}$ cells was twice as high as those of *Apoe*$^{3/3}$ or *Apoe*$^{4/4}$ cells (Figure 1C). In addition, the level of LDLR expression affected the amount of apoE secreted from the cultured primary hepatocytes (Figure 1A). The ratio of medium apoE to cell-associated apoE in the cultured *Apoe*$^{4/4}$*Ldlr*$^{h/+}$ hepatocytes was significantly lower than in *Apoe*$^{4/4}$ cells (Figure 1C). In turn, the ratio in hepatocytes lacking LDLR (*Apoe*$^{4/4}$ *Ldlr*$^{-/-}$) expression was significantly higher than in *Apoe*$^{4/4}$ hepatocytes (Figure 1C). Heparinase treatment increased apoE4 in the medium in both *Apoe*$^{4/4}$*Ldlr*$^{h/+}$ and *Apoe*$^{4/4}$ hepatocytes, but the apoE4 secretion from the *Apoe*$^{4/4}$*Ldlr*$^{h/+}$ remained significantly depressed (Figure 1D). These data indicate that the relative amount of apoE secretion from the liver is inversely related to the affinity of the isoforms to the receptor as well as to the levels of LDLR expression.

The ratio of extracellular to cell-associated apoE amounts is likely determined by the uptake, but could also be attributable to changes in apoE synthesis or degradation. To determine how the LDLR expression levels affect production and degradation of apoE, we used a pulse chase system in primary hepatocytes isolated from *Apoe*$^{4/4}$ and *Apoe*$^{4/4}$*Ldlr*$^{h/+}$ mice. The synthesis during a 30 minute (Figure 1E) pulse was not significantly different between *Apoe*$^{4/4}$ (pixel intensity of 150.2±12.4) and *Apoe*$^{4/4}$*Ldlr*$^{h/+}$ (144.8±5.1) hepatocytes, indicating that a 2.5× higher LDLR expression had no effect on the apoE production rate. Cell-associated apoE retained after a 1-hour chase was more in *Apoe*$^{4/4}$*Ldlr*$^{h/+}$ cells than in *Apoe*$^{4/4}$ cells, but they were not significantly different at 4 hours. However, consistent with the observation described

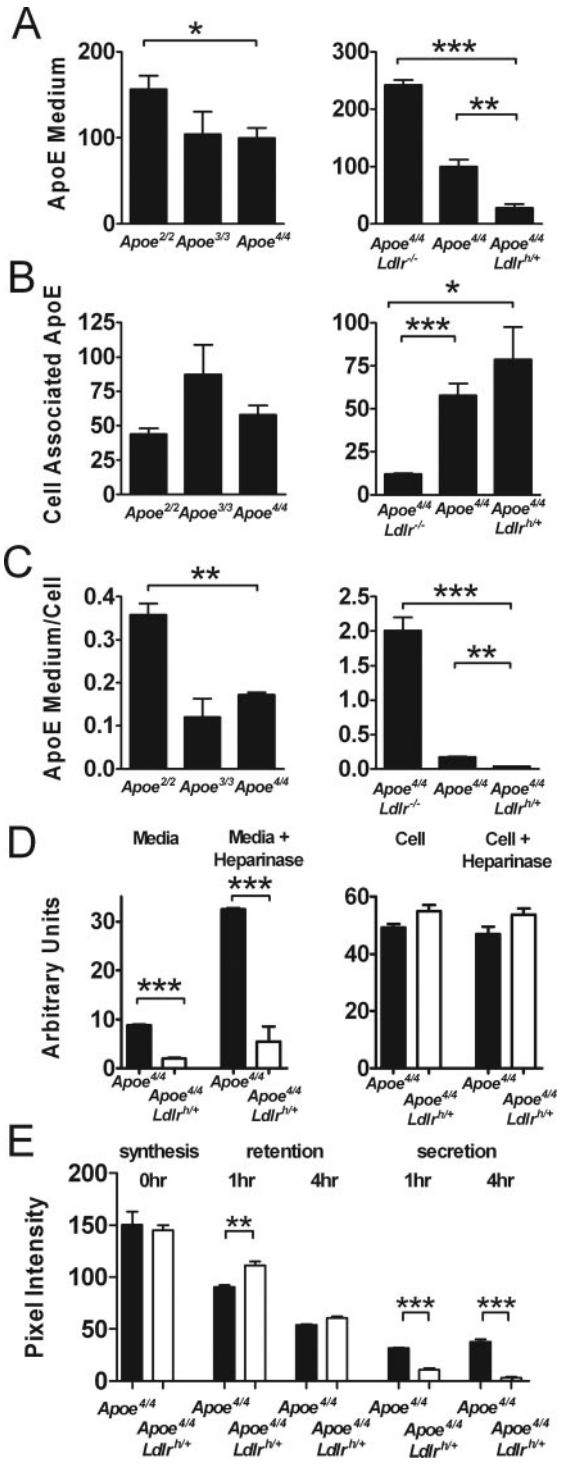

Figure 1. A, Secretion of apoE from primary hepatocytes isolated from *Apoe*$^{2/2}$, *Apoe*$^{3/3}$, *Apoe*$^{4/4}$ (left), and from *Apoe*$^{4/4}$*Ldlr*$^{-/-}$, *Apoe*$^{4/4}$, *Apoe*$^{4/4}$*Ldlr*$^{h/+}$ (right) mice into the culture medium. Cell-associated apoE (B) and the ratio of apoE in the medium/cell-associated (C) from the above primary hepatocytes. D, Effects of heparinase on apoE secretion from *Apoe*$^{4/4}$ and *Apoe*$^{4/4}$*Ldlr*$^{h/+}$ primary hepatocytes. E, Pulse chase analysis of *Apoe*$^{4/4}$ and *Apoe*$^{4/4}$ *Ldlr*$^{h/+}$ hepatocytes. ^{35}S-Methionine in cell-associated apoE (synthesis, time 0) during a 30-minute pulse and after 1-hour and 4-hour chase (retention) and in medium (secretion) was determined using SDS-PAGE and phosphoimager. Values shown are the average of 3 wells. The experiment was repeated with a similar result. $^{**}P \leq 0.005$ and $^{***}P \leq 0.0005$.

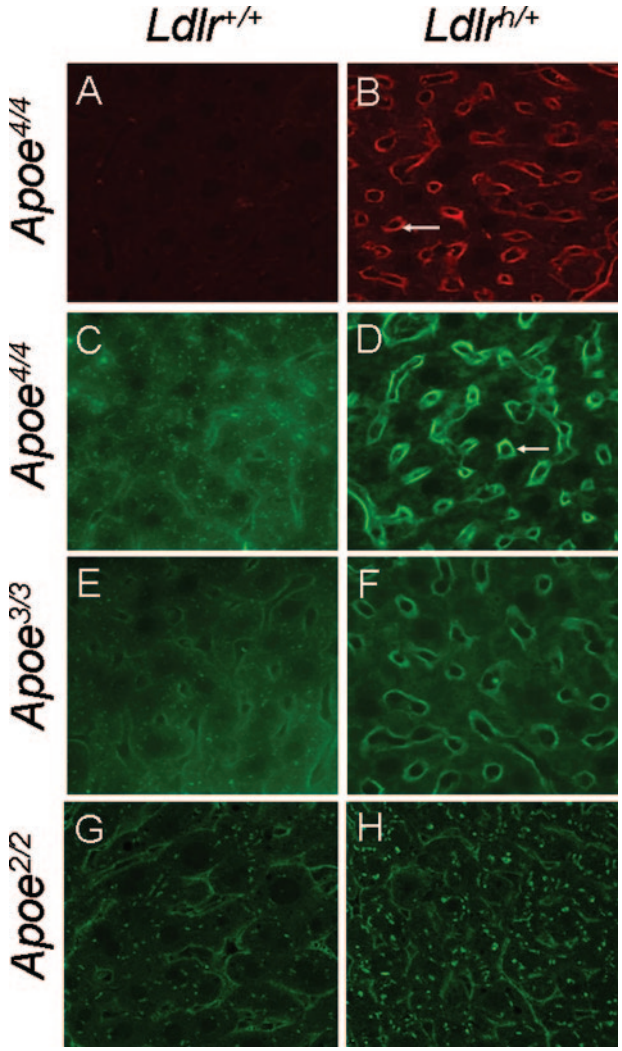

Figure 2. Immunohistochemical localization of apoE in the liver of mice. Anti-human LDLR staining in *Apoe*$^{4/4}$ (A) and *Apoe*$^{4/4}$ *Ldlr*$^{h/+}$ (B). Staining for anti-human apoE in *Apoe*$^{4/4}$ (C), *Apoe*$^{4/4}$ *Ldlr*$^{h/+}$ (D), *Apoe*$^{3/3}$ (E), *Apoe*$^{3/3}$*Ldlr*$^{h/+}$ (F), *Apoe*$^{2/2}$ (G), *Apoe*$^{2/2}$*Ldlr*$^{h/+}$ (H). (600X).

above, apoE4 secreted from *Apoe*$^{4/4}$*Ldlr*$^{h/+}$ cells into the medium was significantly less than that from *Apoe*$^{4/4}$ cells. The sum of the secreted and cell-retained apoE4 in *Apoe*$^{4/4}$ and *Apoe*$^{4/4}$*Ldlr*$^{h/+}$ cells was 81% and 84% at 1 hour and 61% and 44% at 4 hours, respectively, of the initial synthesis suggesting that an elevated LDLR expression also increases apoE4 degradation. The results of experiments with a 60 minute pulse were very similar (supplemental Figure II).

Localization of ApoE Isoforms in the Liver

Immunostaining with an antibody against huLDLR illustrated the sinusoidal localization of the huLDLR in the liver sections of *Apoe*$^{4/4}$*Ldlr*$^{h/+}$ but not in *Apoe*$^{4/4}$ mice (Figure 2A, 2B, and supplemental Figure III). ApoE4 colocalized with the LDLR in the *Apoe*$^{4/4}$*Ldlr*$^{h/+}$ liver as highlighted by the very intense staining of sinusoids with antibody against human apoE (Figure 2D). In contrast, apoE4 staining in the *Apoe*$^{4/4}$ liver was diffuse and also present in the cytoplasm in a punctated pattern (Figure 2C). Very similar staining patterns

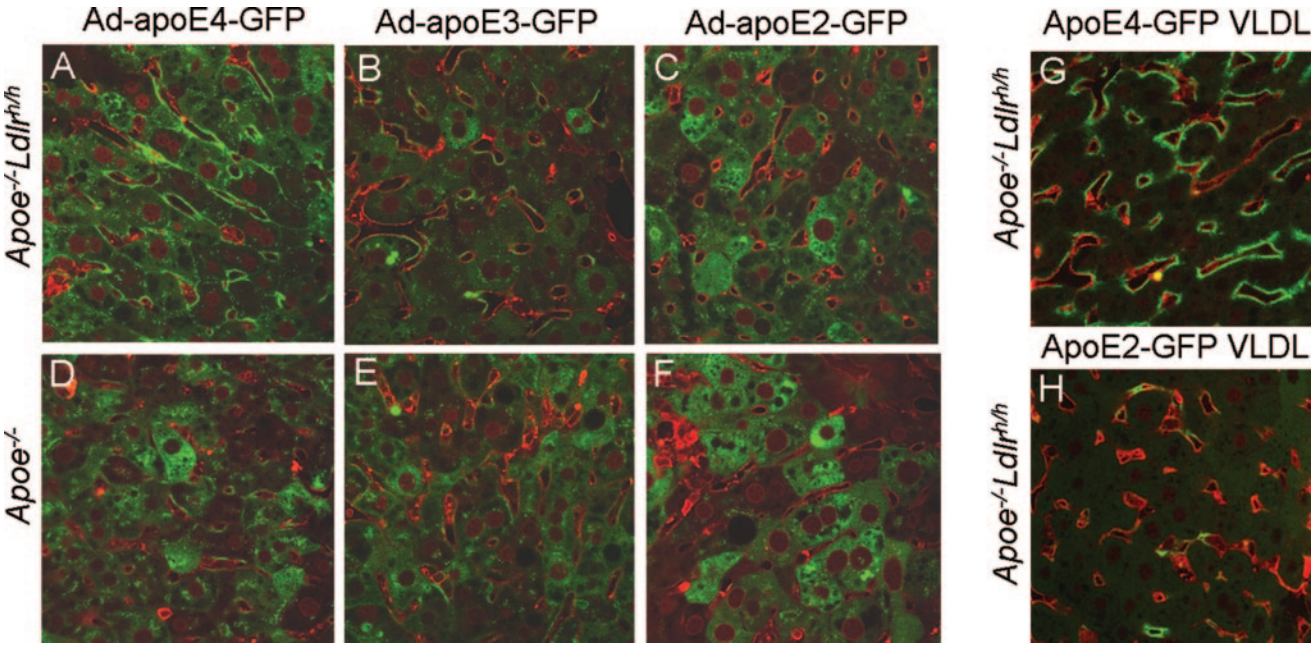

Figure 3. Localization of apoE-GFP fusion proteins in the liver. Ad-apoE4-GFP (A, D), Ad-apoE3-GFP (B, E), and Ad-apoE2-GFP (C, F) were injected into *Apoe*$^{-/-}$Ldlr$^{h/h}$ (A, B, C) and *Apoe*$^{-/-}$ (D, E, F) mice. After 5 days liver sections (100 μm) were stained with Alexafluor633 labeled lectin (red), and GFP (green) signals were examined under a confocal microscopy (600×). VLDL isolated from *Apoe*$^{-/-}$ mice injected with Ad-apoE4-GFP or apoE2-GFP was injected into tail veins of *Apoe*$^{-/-}$Ldlr$^{h/h}$ mice. ApoE4-GFP 5 minutes after i.v. injection (G), and apoE2-GFP (H).

were observed in the livers of *Apoe*$^{3/3}$ and *Apoe*$^{3/3}$*Ldlr*$^{h/+}$ mice (Figure 2E and 2F), except that the sinusoidal staining relative to cytoplasmic staining was less intense in the *Apoe*$^{3/3}$*Ldlr*$^{h/+}$ liver than in the *Apoe*$^{4/4}$*Ldlr*$^{h/+}$ liver. This suggests that the LDLR levels influence sinusoidal localization of apoE4 and, to a lesser extent, of apoE3. *Apoe*$^{2/2}$ and *Apoe*$^{2/2}$*Ldlr*$^{h/+}$ livers both had more pronounced intrahepatic staining than other apoE isoforms (Figure 2G and 2H), and the *Apoe*$^{2/2}$*Ldlr*$^{h/+}$ liver had more intracellular staining than the *Apoe*$^{2/2}$ liver with no increase in sinusoidal staining. Total LDLR proteins in the membrane fraction of *Ldlr*$^{h/+}$ livers detected by Western blots with antibodies specific for human or mouse LDLRs were similar regardless of apoE isoforms (supplemental Figure IV). Absolute amount of each LDLR was not determined.

To confirm the hepatic localization of apoE isoforms and the effect of increased LDLR without using antibodies, we injected Ad-apoE4-GFP, Ad-apoE3-GFP, and Ad-apoE2-GFP into *Apoe*$^{-/-}$ mice. ApoE-GFP fusion proteins appear to function normally and retain isoform specific characteristics as all lowered cholesterol levels in *Apoe*$^{-/-}$ mice (supplemental Figure V). Using confocal microscopy of the liver sections stained with Alexafluor633-labeled lectin to demarcate liver sinusoids, endothelial cells, and the space of Disse (SD),[26] the apoE-GFP fusion proteins were visible as bright green hepatocytes with perinuclear concentration in the cytoplasm of 70% to 80% of the cells (Figure 3A through 3F). Notably, apoE4-GFP and apoE3-GFP also demarked sinusoids. Inspection under a higher magnification revealed that GFP and Alexafluor633 labeled lectin signals were not overlapping (supplemental Figure VI), suggesting that the accumulation of apoE4-GFP is subendothelial in the SD, likely on the hepatocyte surface. The subendothelial accumulation of apoE4-GFP or apoE3-GFP was more pronounced in the liver of the *Apoe*$^{-/-}$Ldlr$^{h/h}$ mice injected with Ad-apoE4-GFP or Ad-apoE3-GFP (Figure 3A and 3B). In marked contrast, Ad-apoE2-GFP showed little accumulation of apoE2-GFP on the hepatocyte surface even in the *Apoe*$^{-/-}$Ldlr$^{h/h}$ mice (Figure 3C). These data demonstrate that the in vivo accumulation of apoE in the SD is dependent on its affinity to the LDLR and the expression levels of the LDLR.

Neither immunostaining nor Ad-apoE-GFP expression allows us to dissociate whether apoE accumulating on the hepatocyte surface is newly synthesized by the hepatocyte or originates from lipoproteins in circulation. However, we note that not all the cells demarcated by intense sinusoidal apoE-GFP signals have strong intracellular GFP signals. This suggests a substantial part of the apoE-GFP may be derived from apoE-GFP synthesized by other transfected hepatocytes. To confirm this, we isolated VLDL fractions enriched with apoE2-GFP or apoE4-GFP from *Apoe*$^{-/-}$*Ldlr*$^{-/-}$ mice 5 days after transfection with the Ad-apoE2-GFP or Ad-apoE4-GFP, and injected them into *Apoe*$^{-/-}$Ldlr$^{h/h}$ mice. When livers were examined under confocal microscopy 5 minutes after the injection through tail veins, apoE4-GFP was already localized on hepatocyte surfaces (Figure 3G). This suggests that lipoproteins that acquire apoE4 during the circulation can accumulate in the SD very efficiently. In contrast, very little apoE2-GFP was accumulated on the hepatocyte surface during this time (Figure 3H).

Sinusoidal Sequestration of ApoE and Internalization of Lipoprotein Remnants

The striking differences in the cellular localizations of the different apoE isoforms in the livers of mice with high levels

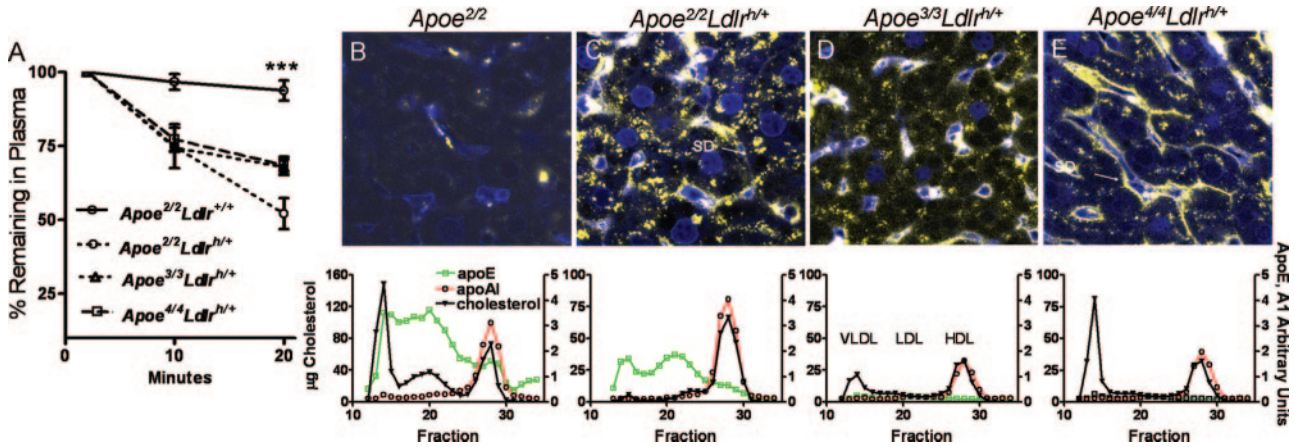

Figure 4. Localization and clearance of VLDL. A, DiI-labeled *Apoe*$^{-/-}$ VLDL was injected into *Apoe*$^{2/2}$, *Apoe*$^{2/2}$*Ldlr*$^{h/+}$, *Apoe*$^{3/3}$*Ldlr*$^{h/+}$, and *Apoe*$^{4/4}$*Ldlr*$^{h/+}$ mice and fluorescent signals in plasma were measured at 2, 10, and 20 minutes. 2 minutes was taken as 100% (n=4). B through E, Livers at 20 minutes were analyzed by confocal microscopy for DiI-VLDL (yellow) and Alexafluor633 labeled lectin (blue): *Apoe*$^{2/2}$ (B), *Apoe*$^{2/2}$*Ldlr*$^{h/+}$ (C), *Apoe*$^{3/3}$*Ldlr*$^{h/+}$ (D), *Apoe*$^{4/4}$*Ldlr*$^{h/+}$ (E). Below each panel are their lipoprotein profiles. Cholesterol (black), and relative amounts of apoE (green) and apoA1 (red) in the lipoproteins separated by fast protein liquid chromatography (FPLC) from plasma of mice before the injection of DiI-labeled VLDL.

of LDLR expression raise a question regarding the physiological relevance of apoE accumulated on the sinusoidal surface to remnant clearance. We therefore examined how the apoE isoforms affect plasma VLDL clearance and liver uptake by injecting DiI-labeled *Apoe*$^{-/-}$ VLDL into *Apoe*$^{2/2}$, *Apoe*$^{2/2}$*Ldlr*$^{h/+}$, *Apoe*$^{3/3}$*Ldlr*$^{h/+}$, and *Apoe*$^{4/4}$*Ldlr*$^{h/+}$ mice. Decay of DiI-labeled *Apoe*$^{-/-}$ VLDL particles from plasma showed that the *Apoe*$^{2/2}$ mice had the slowest clearance of *Apoe*$^{-/-}$ VLDL (Figure 4A). The clearance in the *Apoe*$^{2/2}$*Ldlr*$^{h/+}$, *Apoe*$^{3/3}$*Ldlr*$^{h/+}$, and *Apoe*$^{4/4}$*Ldlr*$^{h/+}$ mice were not different at 10 minutes after injection. However, the VLDL was removed from circulation during the next 10 minutes significantly faster in the *Apoe*$^{2/2}$*Ldlr*$^{h/+}$ mice than in both *Apoe*$^{3/3}$*Ldlr*$^{h/+}$ and *Apoe*$^{4/4}$*Ldlr*$^{h/+}$mice. At 20 minutes after injection, DiI-VLDL was barely detectable in the liver of *Apoe*$^{2/2}$ mice (Figure 4B), but was avidly internalized in the *Apoe*$^{2/2}$*Ldlr*$^{h/+}$ liver (Figure 4C). Most of the signal was intracellular and surface-bound DiI-VLDL was negligible (arrow, SD). In marked contrast, strong DiI-signal was on the hepatic surface of the *Apoe*$^{4/4}$*Ldlr*$^{h/+}$ liver (arrow, SD), whereas intracellular DiI-VLDL was less than in the *Apoe*$^{2/2}$*Ldlr*$^{h/+}$ liver (Figure 4C and 4E). Heparinase treatment of the *Apoe*$^{4/4}$*Ldlr*$^{h/+}$ mice 5 minutes before the injection of DiI-VLDL did not alter the localization of apoE and VLDL appreciably (supplemental Figure VII).

The reduced ability to internalize VLDL by the liver was associated with the accumulation of cholesterol-rich but apoE-poor VLDL remnants and 10-fold less total apoE in the plasma of *Apoe*$^{4/4}$*Ldlr*$^{h/+}$ mice compared to the *Apoe*$^{2/2}$*Ldlr*$^{h/+}$ mice (Figure 4B through 4E, lower panels). Plasma apoprotein to lipid ratios indicate that the *Apoe*$^{2/2}$*Ldlr*$^{h/+}$ mice have the most apoE enriched lipoproteins in all subclasses. Consistent with their higher HDL-C, *Apoe*$^{2/2}$*Ldlr*$^{h/+}$ mice also had more plasma apoA1 than *Apoe*$^{4/4}$*Ldlr*$^{h/+}$ mice, but the ratios of cholesterol to apoA1 in the HDL particles in these mice were not different. Hepatic expression of apoE, LRP, and SRB-1 that could influence lipid/cholesterol flux were not significantly different among experimental mice (supplemental Figure VIII).

Taken together, these data demonstrate that apoE2, which is elevated in the plasma on circulating lipoproteins and minimally associated with the hepatocyte surface, can facilitate internalization of apoE$^{-/-}$ VLDL remnants in the mice expressing a high level of LDLR. In contrast, apoE4 that is accumulated on the hepatocyte surface appears to enhance sequestration of VLDL remnants, but has only a limited capacity to participate in the internalization of lipoprotein remnants.

Discussion

There is little debate that the LDLR is important for clearance of remnant lipoproteins under normal physiological conditions, and that this process is mediated by the high-affinity binding of multiple apoE proteins on a lipoprotein particle to the LDLR.[3] However, the common apoE isoforms in humans having affinities for the LDLR in the order of apoE4>apoE3>apoE2 significantly impact plasma cholesterol levels in an inverse order in humans and in mouse models.[2,10,13,14,17,18,27] Our current study using humanized mice provides evidence that the extent of localization of the human apoE-isoforms in the liver inversely correlates with their efficacy in lipoprotein remnant internalization in vivo.

Previous studies have demonstrated the presence of apoE immunoreactivity along the sinusoidal front of hepatocytes together with some punctate cytoplasmic staining in the liver of wild type rats and mice.[4,28,29] Studies have also shown that apoE is clustered on hepatocyte microvilli projecting into the space of Disse of the rat liver,[28] and are used for hepatic endocytosis of remnants.[4] Also, liver-derived and localized apoE has been shown to be more effective than nonhepatic derived apoE in the receptor-mediated internalization of remnants by the liver.[30–32] Similarly, Linton et al showed in the space of Disse of the *Apoe*$^{-/-}$*Ldlr*$^{-/-}$ mice that received wild-type bone marrows that an intense immunoreactivity for extrahepatic apoE was present on the cell surface but cyto-

plasmic staining was not detected, indicating that no uptake of apoE-containing lipoproteins was occurring.[29] These observations, using wild-type rodent apoE, clearly underscore the important role of apoE localized in the sinusoids of the liver in remnant uptake.

Multiple experiments have also shown that a substantial amount of apoE internalized with TRLs by the liver are recycled back to the cell-surface and resecreted, and that this resecretion is isoform specific.[33–35] Considering that apoE4 and apoE3 have a higher affinity to the LDLR, our results showing enhanced accumulation of apoE4 and apoE3 in the space of Disse compared to apoE2 in mice overexpressing the human LDLR are not surprising. Although absolute amount of LDLR protein in the liver in these mice has not been determined, previous experiments by us and by others have unequivocally shown that the increases in LDLR expression lead to lowering of plasma cholesterol in mice.[36,37] Surprisingly, this surface sequestration of apoE4 does not directly translate to enhanced internalization of VLDL remnants into the cells. Thus, we observed that internalization of DiI-labeled VLDL was slower in the *Apoe*$^{4/4}$*Ldlr*$^{h/+}$ mice than in the *Apoe*$^{2/2}$*Ldlr*$^{h/+}$ mice. Remarkably, there were no indications that the increased LDLR enhances either LDLR-mediated or LDLR-independent uptake of TRL in the *Apoe*$^{4/4}$ *Ldlr*$^{h/+}$ mice. Although we cannot eliminate the possibility that the DiI-labeled VLDL may have exchanged with the plasma lipoproteins in the recipient mice before it reached their hepatic surface, our results suggest that the sinusoidal enrichment of apoE does not necessarily ensure that apoE is transferred to TRL particles.

Jones et al recently demonstrated that mice with mutations in an adaptor protein involved in LDLR internalization can still clear VLDL.[38] The authors suggested the possibility that VLDL remnants bind the LDLR on the hepatocyte cell surface but that their internalization may be mediated by another cell surface component that is also independent of LRP or HSPG. Although the nature of this process is yet to be elucidated, the concept that remnants are handed from one cell surface molecule to the other while accumulating apoE molecules before their final internalization is attractive. Because LDLR serves as a regulator of apoE availability more than just a receptor, a higher affinity of apoE4 to the LDLR could delay the handing-off process, and thereby delay the clearance of remnants in the *Apoe*$^{4/4}$*Ldlr*$^{h/+}$ mice. In contrast, the reduced affinity of apoE2 for the LDLR, and to a lesser extent for HSPG, results in limited apoE2 sequestration on the surface of hepatocytes allowing their secretion into the circulation.[39] As circulating lipoproteins in the *Apoe*$^{2/2}$*Ldlr*$^{h/+}$ mice have high apoE contents, a significant portion of the apoE2-enrichment of remnants may take place in the circulation and contribute to the subsequent remnant clearance in the liver of these mice. (A hypothetical model of interactions between apoE2 and apoE4 with the LDLR within the sinusoidal space is presented in supplemental Figure IX).

The genetic interaction between the apoE-isoforms and LDLR gene expression observed in mice translates well to humans, although not completely. For instance humans with APOE*4 have elevated LDL remnants and *Apoe*$^{4/4}$*Ldlr*$^{h/+}$ mice accumulate VLDL remnants.[12] Nevertheless, an enhanced sequestration but delayed clearance of VLDL could prolong their exposure to surface bound lipases which could then accelerate lipolysis and conversion of VLDL to smaller remnants in the livers expressing apoE4 of both species. In contrast, limited interaction of apoE2 with the LDLR enhances VLDL clearance and reduces remnant production in apoE2 livers.[21,40] Consequently, the overall degrees of reduction in LDL-cholesterol resulting from the increase in LDLR expression in humans is likely to be apoE-isoform–dependent; with more pronounced reduction in individuals with apoE2 but lesser reduction with apoE4.

Acknowledgments

We thank Dr Robert Bagnell for help with microscopy and image acquisition and Svetlana Zihilcheva for technical help.

Sources of Funding

This work was supported by a grant HL42630. M.A. was supported by T32HL69768.

Disclosures

None.

References

1. Mahley RW. Apolipoprotein E: cholesterol transport protein with expanding role in cell biology. *Science*. 1988;240:622–630.
2. Mahley RW, Rall SC Jr. Apolipoprotein E. far more than a lipid transport protein. *Annu Rev Genomics Hum Genet*. 2000;1:507–537.
3. Mahley RW, Huang Y. Atherogenic remnant lipoproteins: role for proteoglycans in trapping, transferring, and internalizing. *J Clin Invest*. 2007;117:94–98.
4. Shimano H, Namba Y, Ohsuga J, Kawamura M, Yamamoto K, Shimada M, Gotoda T, Harada K, Yazaki Y, Yamada N. Secretion-recapture process of apolipoprotein E in hepatic uptake of chylomicron remnants in transgenic mice. *J Clin Invest*. 1994;93:2215–2223.
5. Weisgraber KH, Innerarity TL, Mahley RW. Abnormal lipoprotein receptor-binding activity of the human E apoprotein due to cysteine-arginine interchange at a single site. *J Biol Chem*. 1982;257:2518–2521.
6. Bohnet K, Pillot T, Visvikis S, Sabolovic N, Siest G. Apolipoprotein (apo) E genotype and apoE concentration determine binding of normal very low density lipoproteins to HepG2 cell surface receptors. *J Lipid Res*. 1996;37:1316–1324.
7. Knouff C, Hinsdale ME, Mezdour H, Altenburg MK, Watanabe M, Quarfordt SH, Sullivan PM, Maeda N. Apo E structure determines VLDL clearance and atherosclerosis risk in mice. *J Clin Invest*. 1999;103:1579–1586.
8. Schneider WJ, Kovanen PT, Brown MS, Goldstein JL, Utermann G, Weber W, Havel RJ, Kotite L, Kane JP, Innerarity TL, Mahley RW. Familial dysbetalipoproteinemia. Abnormal binding of mutant apoprotein E to low density lipoprotein receptors of human fibroblasts and membranes from liver and adrenal of rats, rabbits, and cows. *J Clin Invest*. 1981;68:1075–1085.
9. Mamotte CD, Sturm M, Foo JI, van Bockxmeer FM, Taylor RR. Comparison of the LDL-receptor binding of VLDL and LDL from apoE4 and apoE3 homozygotes. *Am J Physiol*. 1999;276:E553–E557.
10. Gylling H, Kontula K, Miettinen TA. Cholesterol absorption and metabolism and LDL kinetics in healthy men with different apoprotein E phenotypes and apoprotein B Xba I and LDL receptor Pvu II genotypes. *Arterioscler Thromb Vasc Biol*. 1995;15:208–213.
11. Curtiss LK, Boisvert WA. Apolipoprotein E and atherosclerosis. *Curr Opin Lipidol*. 2000;11:243–251.
12. Davignon J, Gregg RE, Sing CF. Apolipoprotein E polymorphism and atherosclerosis. *Arteriosclerosis*. 1988;8:1–21.
13. Gregg RE, Zech LA, Schaefer EJ, Stark D, Wilson D, Brewer HB Jr. Abnormal in vivo metabolism of apolipoprotein E4 in humans. *J Clin Invest*. 1986;78:815–821.
14. Boerwinkle E, Utermann G. Simultaneous effects of the apolipoprotein E polymorphism on apolipoprotein E, apolipoprotein B, and cholesterol metabolism. *Am J Hum Genet*. 1988;42:104–112.

15. Sullivan PM, Mezdour H, Aratani Y, Knouff C, Najib J, Reddick RL, Quarfordt SH, Maeda N. Targeted replacement of the mouse apolipoprotein E gene with the common human APOE3 allele enhances diet-induced hypercholesterolemia and atherosclerosis. *J Biol Chem*. 1997;272:17972–17980.
16. Sullivan PM, Mezdour H, Quarfordt SH, Maeda N. Type III hyperlipoproteinemia and spontaneous atherosclerosis in mice resulting from gene replacement of mouse Apoe with human Apoe*2. *J Clin Invest*. 1998; 102:130–135.
17. Knouff C, Malloy S, Wilder J, Altenburg MK, Maeda N. Doubling expression of the low density lipoprotein receptor by truncation of the 3′-untranslated region sequence ameliorates type III hyperlipoproteinemia in mice expressing the human apoe2 isoform. *J Biol Chem*. 2001; 276:3856–3862.
18. Malloy SI, Altenburg MK, Knouff C, Lanningham-Foster L, Parks JS, Maeda N. Harmful effects of increased LDLR expression in mice with human APOE*4 but not APOE*3. *Arterioscler Thromb Vasc Biol*. 2004; 24:91–97.
19. Altenburg MK, Johnson LA, Wilder JC, Maeda N. Apolipoprotein E4 in macrophages enhances atherogenesis in an LDL receptor dependent manner. *J Biol Chem*. 2007.
20. Lucic D, Huang ZH, Gu de S, Altenburg MK, Maeda N, Mazzone T. Regulation of macrophage apoE secretion and sterol efflux by the LDL receptor. *J Lipid Res*. 2007;48:366–372.
21. van Dijk KW, van Vlijmen BJ, de Winther MP, van 't Hof B, van der Zee A, van der Boom H, Havekes LM, Hofker MH. Hyperlipidemia of ApoE2(Arg(158)-Cys) and ApoE3-Leiden transgenic mice is modulated predominantly by LDL receptor expression. *Arterioscler Thromb Vasc Biol*. 1999;19:2945–2951.
22. Farkas MH, Swift LL, Hasty AH, Linton MF, Fazio S. The recycling of apolipoprotein E in primary cultures of mouse hepatocytes. Evidence for a physiologic connection to high density lipoprotein metabolism. *J Biol Chem*. 2003;278:9412–9417.
23. Dekroon RM, Armati PJ. Endocytosis of apoE-EGFP by primary human brain cultures. *Cell Biol Int*. 2002;26:761–770.
24. Stephan ZF, Yurachek EC. Rapid fluorometric assay of LDL receptor activity by DiI-labeled LDL. *J Lipid Res*. 1993;34:325–330.
25. Lorenz JN, Gruenstein E. A simple, nonradioactive method for evaluating single-nephron filtration rate using FITC-inulin. *Am J Physiol*. 1999;276: F172–F177.
26. Kawakami H, Hirano H. Lectin-binding patterns on the plasma membranes of dissociated rat liver cells. *Histochemistry*. 1984;80:415–420.
27. Gregg RE, Zech LA, Brewer HB Jr. Apolipoprotein E alleles in severe hypertriglyceridaemia. *Lancet*. 1983;1:353.
28. Hamilton RL, Wong JS, Guo LS, Krisans S, Havel RJ. Apolipoprotein E localization in rat hepatocytes by immunogold labeling of cryothin sections. *J Lipid Res*. 1990;31:1589–1603.
29. Linton MF, Hasty AH, Babaev VR, Fazio S. Hepatic apo E expression is required for remnant lipoprotein clearance in the absence of the low density lipoprotein receptor. *J Clin Invest*. 1998;101:1726–1736.
30. Raffai RL, Hasty AH, Wang Y, Mettler SE, Sanan DA, Linton MF, Fazio S, Weisgraber KH. Hepatocyte-derived ApoE is more effective than non-hepatocyte-derived ApoE in remnant lipoprotein clearance. *J Biol Chem*. 2003;278:11670–11675.
31. Cooper AD. Hepatic uptake of chylomicron remnants. *J Lipid Res*. 1997; 38:2173–2192.
32. Yu KC, Jiang Y, Chen W, Cooper AD. Rapid initial removal of chylomicron remnants by the mouse liver does not require hepatically localized apolipoprotein E. *J Lipid Res*. 2000;41:1715–1727.
33. Heeren J, Grewal T, Jackle S, Beisiegel U. Recycling of apolipoprotein E and lipoprotein lipase through endosomal compartments in vivo. *J Biol Chem*. 2001;276:42333–42338.
34. Heeren J, Grewal T, Laatsch A, Becker N, Rinninger F, Rye KA, Beisiegel U. Impaired recycling of apolipoprotein E4 is associated with intracellular cholesterol accumulation. *J Biol Chem*. 2004;279: 55483–55492.
35. Swift LL, Farkas MH, Major AS, Valyi-Nagy K, Linton MF, Fazio S. A recycling pathway for resecretion of internalized apolipoprotein E in liver cells. *J Biol Chem*. 2001;276:22965–22970.
36. Herz J, Gerard RD. Adenovirus-mediated transfer of low density lipoprotein receptor gene acutely accelerates cholesterol clearance in normal mice. *Proc Natl Acad Sci U S A*. 1993;90:2812–2816.
37. Yokode M, Hammer RE, Ishibashi S, Brown MS, Goldstein JL. Diet-induced hypercholesterolemia in mice: prevention by overexpression of LDL receptors. *Science*. 1990;250:1273–1275.
38. Jones C, Garuti R, Michaely P, Li WP, Maeda N, Cohen JC, Herz J, Hobbs HH. Disruption of LDL but not VLDL clearance in autosomal recessive hypercholesterolemia. *J Clin Invest*. 2007;117:165–174.
39. Ji ZS, Fazio S, Mahley RW. Variable heparan sulfate proteoglycan binding of apolipoprotein E variants may modulate the expression of type III hyperlipoproteinemia. *J Biol Chem*. 1994;269:13421–13428.
40. Huang Y, Liu XQ, Rall SC Jr, Mahley RW. Apolipoprotein E2 reduces the low density lipoprotein level in transgenic mice by impairing lipoprotein lipase-mediated lipolysis of triglyceride-rich lipoproteins. *J Biol Chem*. 1998;273:17483–17490.

Supplemental Materials for

Human LDL Receptor Enhances Sequestration of ApoE4 and VLDL Remnants on the Surface of Hepatocytes but not their Internalization in Mice

Michael Altenburg, Jose Arbones-Mainar, Lance Johnson, Jennifer Wilder, and Nobuyo Maeda

Department of Pathology and Laboratory Medicine, The University of North Carolina at Chapel Hill, Chapel Hill, North Carolina 27599-7525, USA

Detailed Methods

Quantitation of apoE and apoA1. ApoE and apoA1 content in lipoprotein fractions were quantified by an antigen capture enzyme-linked immunosorbent assay (ELISA), using a 1:10000 dilution of 1.5 mg/ml mouse monoclonal anti-human apoE antibody (Calbiochem) or rabbit anti mouse apoA1 antiserum (gift from Dr. H. deSilva) as described.[1]

Adenoviruses. Plasmid vectors containing cytomegalus viral promoter-driven cDNA for fusion proteins, ApoE2-GFP, apoE3-GFP, and apoE4-GFP, were provided by Dr. Robert DeKroon at Duke University. These vectors express fusion proteins with EGFP (enhanced green fluorescent protein) attached to the C terminal end of each apoE isoform.[2] Adenoviral vectors encoding apoE2-GFP, apoE3-GFP, and apoE4-GFP were made using the AdEasy adenoviral system (Stratagene) according to the manufacturer's instructions. Ad-apoE-GFP's were amplified in 293 cells, purified by CsCl density gradient ultracentrifugation and dialyzed against 10 mM Tris pH 8.0, 2mM MgCl2, 4% sucrose. Recombinant adenovirus stock stored at –80 °C was diluted with PBS and $1x10^9$ PFU in 0.2 ml of adenovirus was injected into a mouse via tail vein.

Culture of primary mouse hepatocytes. Mice were anesthetized using 2,2,2-tribromoethanol, the portal vein was cannulated with a 24-gauge plastic cannula, and the liver was perfused with Ca^{2+}/Mg^{2+}-free Hanks' Balanced Salt Solution containing glucose (10 mM) and HEPES (10 mM) at a flow rate of 3 ml/min for 10 min. The perfusion was continued for another 10 min with the same solution containing collagenase (0.05%, type I, Sigma). The liver was removed from the animal, minced in phosphate buffered saline (PBS), and the dissociated cells were dispersed by shaking followed by filtration through 100-µm nylon cell strainers (Falcon). The liver capsule and dish were rinsed in Dulbecco's modified Eagle's medium (DMEM) containing 0.02 µg/ml dexamethasone, 100 units/ml of penicillin and 100 µg/ml of streptomycin. The cells were pelleted by gravity sedimentation in Percoll for 5 min. at 4 °C. The medium was aspirated, leaving 5 ml total volume, and fresh medium was added to 10 ml. The cells were resuspended and viability was assessed by trypan blue exclusion. The yield of hepatocytes ranged from $3x10^6$ to $6x10^6$ cells/g of liver, and viability was greater than 80%. The cells were plated onto 60-mm mouse collagen IV-coated dishes (Falcon) at a density of $1.2x10^6$ viable cells/dish in 2 ml of the above medium containing 10% FBS unless otherwise stated.

Plasma lipoprotein analysis, DiI labeling and injection. Plasma was isolated and total cholesterol and triglycerides were measured as described.[3] Pooled plasma samples (100µL) were fractionated by fast protein liquid chromatography (FPLC) using a Superose 6 HR10/30 column (Pharmacia Biotech Inc). The VLDL fraction was isolated from pooled plasma by ultracentrifugation at d<1.006 g/ml and labeled with 1,1′-dioctadecyl-3,3,3′,3′-tetramethylindocarbocyanine perchlorate (DiI C_{18}; Molecular Probes Inc.), as described by Stephan and Yurachek.[4] DiI-labeled VLDL (100 µg protein) was injected into tail veins of mice, and livers were fixed with 4% paraformaldehyde either 10 or 20 min later. DiI-labeled VLDL remaining in the plasma was determined using a microscope fluorometer (Olympus FV500 with a SPOT 2 digital camera) at 2min, 10 min, and 20 min using a modification of the fluorometric procedure described by Lorenze et al.[5]

Immunohistochemistry and confocal microscopic analyses. Animals were given a lethal overdose of 2, 2, 2-tribromoethanol. Livers were perfused through the portal vein at 2 ml/min for 2 min with 4% paraformaldehyde, excised from animals and further fixed overnight in 4% paraformaldehyde. Slides with consecutive liver paraffin sections (5µm) were incubated overnight at 4 °C with either goat anti-human apoE or goat anti-LDLR antibodies (1:1000, Calbiochem) followed by an incubation with FITC conjugated anti-goat IgG (1:500, Santa Cruz). Slides were cover slipped after application of Vectashield anti-fade mounting medium (Vector H-1000, Vector Laboratories) and were observed with an IX70 inverted microscope (Olympus) equipped with a filter set for FITC (exciter 560/55, dichroic 595, emitter 645/75, Chroma Technology Corp). Images were captured with a SPOT 2 digital camera (Diagnostic Instruments) and analyzed with SPOT version 4.0.9 (Diagnostic Instruments) and ImageJ 1.33u (NIH) software. For confocal microscopic analysis of apoE-GFP in fixed tissues, 50 or 100 µm-thick sections were cut with a vibratome and stored free-floating in PBS at 4º C. Before analyses with an Olympus FV500 confocal microscope, individual sections were treated with sodium borohydride (1mg/ml in PBS) for 30 minutes at room temperature, and then washed in PBS three times for five minutes each at room temperature to reduce fixative-induced fluorescence. Individual vibratome sections were also stained with AlexaFluor633 labeled Wheat germ agglutinin (WGA) (50 micrograms/ml) for 30 min. For GFP fluorescence, the 488 line of an Argon laser was used for excitation and the 505 to 525 nm band-pass filter for emission. To acquire labeled WGA images for endothelial cell staining, the 633 line of a Helium/Neon-red laser was used for excitation and the 660 band-pass filter for emission (Cy5). GFP and Alexaflour633 fluorescence images were scanned independently with only their respective excitation and emission frequencies to eliminate bleed through. To acquire DiI labeled images for VLDL uptake, the 543 nm line of a Helium/Neon-green laser was used for excitation and the 560-600 band-pass filter for emission (DiI).

Gene Expression. RNA was extracted using RNAeasy kit (Qiagen, Valencia, CA) according to the manufacturer's protocol from livers of mice that were fed a HFW diet for 2 weeks. Real time RT-PCR amplifications were performed in a 96-well plate in the ABI Prism 7700 sequence detector (PE Biosystems) in a total volume of 30 µl, which included 10 µl of RNA sample from the ABI Prism 6700 plus 20 µl of a reaction mixture. Each RT-PCR amplification was performed in duplicate: 30 min at 48 °C for the RT reaction and then 10 min at 94 °C, followed by a total of 40 temperature cycles (15sec at 94 °C and 1 min at 60 °C). To determine total *Ldlr* mRNA levels, a primer probe system specific for murine exon 1, which is also present in mice targeted for the *huLDLR*, was used.[6]

Liver membrane isolation and Western Blotting for LDLR. Livers were removed and transferred to 5 ml of an ice-cold solution of 0.25 M sucrose, 0.1 M Tris, and protease inhibitors (200mM PMSF, leupeptin, aprotinin), pH 7.4. The livers were homogenized and spun at 10000 × *g* for 10 min to pellet cell debris and nuclei. The supernatant was centrifuged at 100,000 × *g* for 30 min. The resulting membrane containing pellet was resuspended in 0.5 ml of Tris-buffered saline TBS with protease inhibitors, using a 22 gauge needle. The second supernatant was centrifuged again at 100,000 × *g* for 30 min and the pellet was resuspended in 100ul of TBS. 10 µg of protein as determined by Bradford Assay (Bio-Rad) was run on a 4-20% pre-cast gradient gel (NuSep) and transferred to an Immobilon –P membrane (millipore). Anti HuLDLR (Fitzgerald Industries International) and Anti Mouse LDLR (R&D sytstems) as well as horseradish peroxidase conjugated secondary antibodies were used at a 1:10000 dilution. After washing 4X 10 min in TBS-Tween, blots were developed with ECL reagent (Amersham) and exposed to Film (Kodak).

Heparin and Heparinase treatments and injections. Mice were injected via the tail vein with heparinase (30U/mouse; Sigma). Five min after heparinase injection mice, were injected via tail vein with 100 µg DiI labeled Eko VLDL and blood was collected after 2, 5, 10, and 20 min. Primary hepatocytes were treated with 3U/ml Heparinase (Sigma) for 1hour.

Supplemental Table 1 Description of mice used in the work.

Supplemental Table 1

Mice Genotype	Abb.	Description
Apoe$^{2/2}$	2m	human apoE2 C57BL/6
Apoe$^{2/2}$ *Ldlr*$^{h/+}$	2h	human apoE2 and increased LDLR C57BL/6
Apoe$^{3/3}$	3m	human apoE3 C57BL/6
Apoe$^{3/3}$ *Ldlr*$^{h/+}$	3h	human apoE3 and increased LDLR C57BL/6
Apoe$^{4/4}$	4m	human apoE4 C57BL/6
Apoe$^{4/4}$ *Ldlr*$^{h/+}$	4h	human apoE4 and increased LDLR C57BL/6
Apoe$^{4/4}$ *Ldlr*$^{-/-}$	4ko	human apoE4 and no LDLR C57BL/6
Apoe$^{-/-}$	Eko	no apoE C57BL/6
Apoe$^{-/-}$ *Ldlr*$^{h/h}$	Eh	no apoE and increased LDLR (homozygous) C57BL/6
Ldlr$^{-/-}$	ll	no LDLR C57BL/6
Ldlr$^{h/h}$	hh	increased LDLR (homozygous) C57BL/6

Supplemental Figure I.

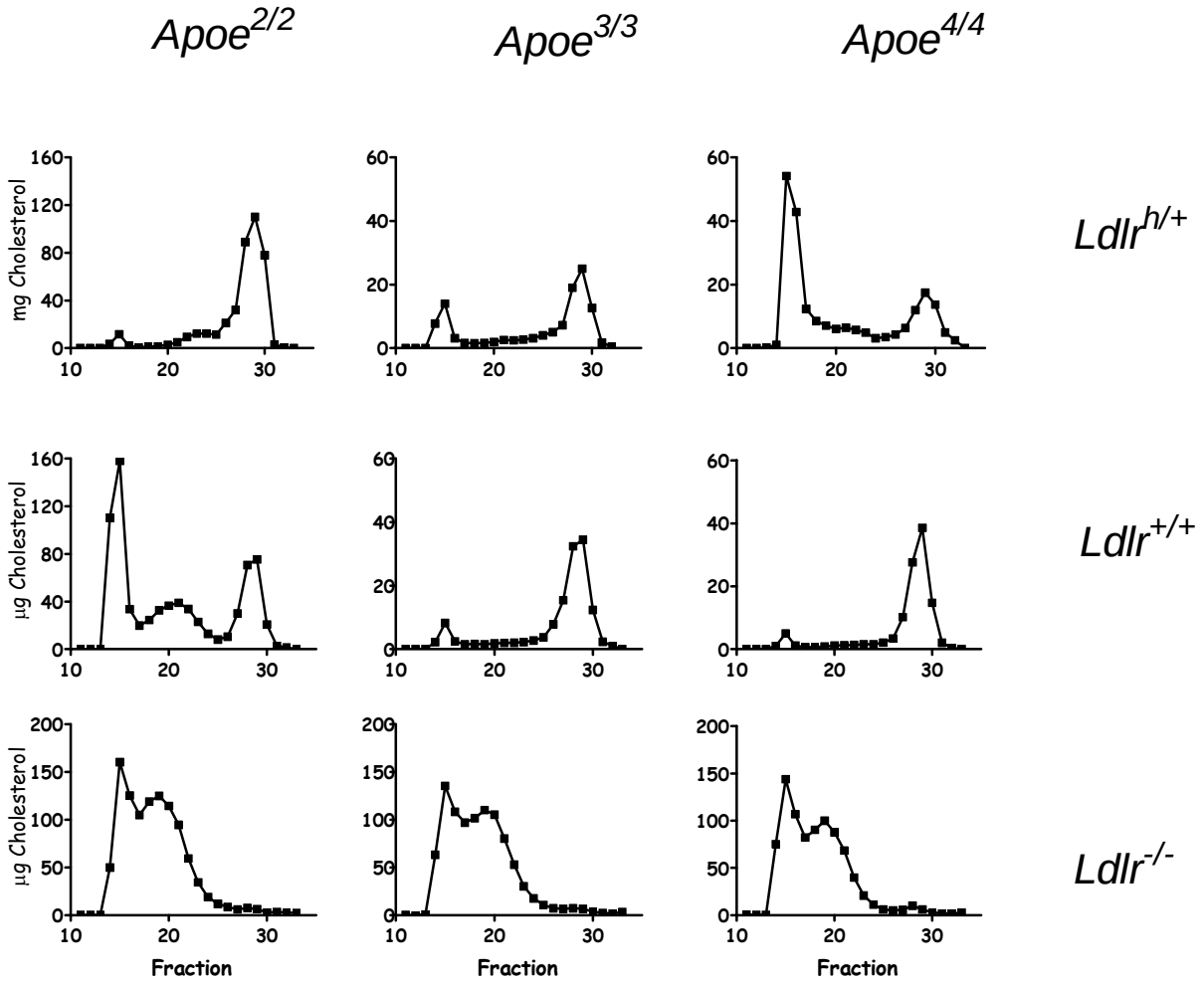

Supplemental Figure I. *Lipoprotein distribution in mice with human apoE*. Mice expressing apoE2 (left), apoE3 (center) and apoE4 (right) with no LDLR (*Ldlr*$^{-/-}$, bottom), wildtype (*Ldlr*$^{+/+}$, center), and overexpression of the LDLR (*Ldlr*$^{h/+}$, top) were on a HFW diet. Plasma lipoproteins were separated by FPLC and cholesterol in each fraction is shown. VLDL, fractions 14-16; LDL, fractions 19-23; HDL, fractions 26-30.

Supplemental Figure II.

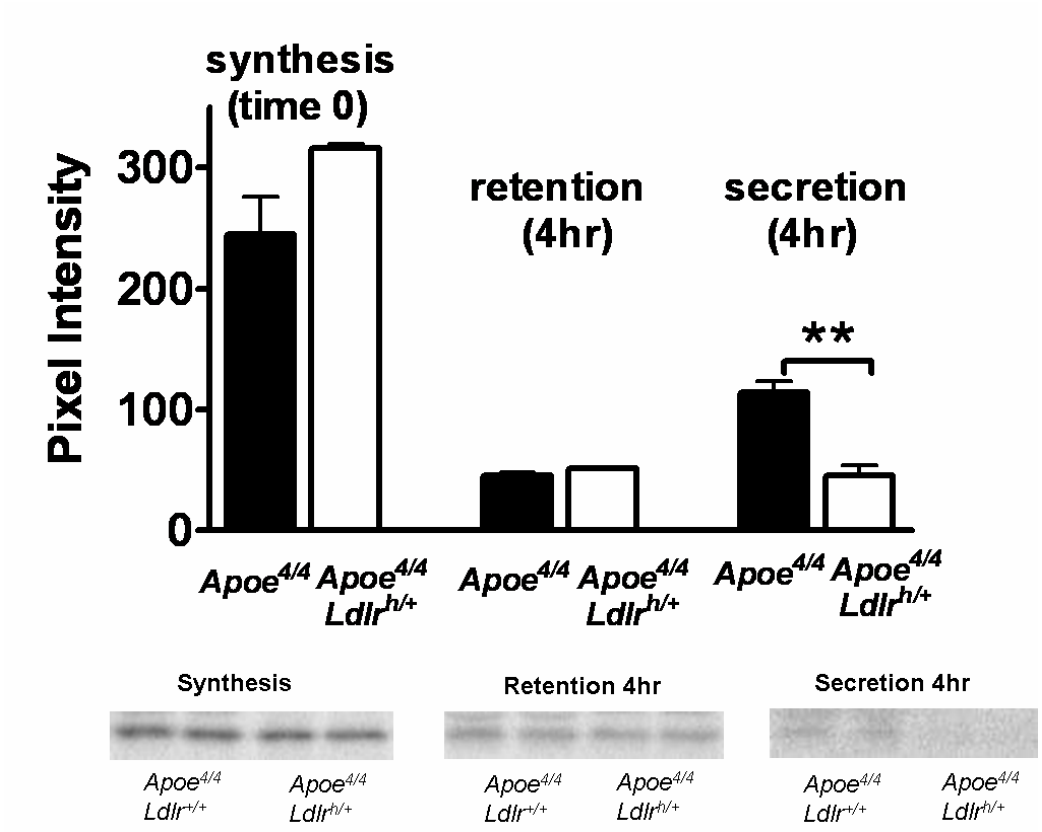

Supplemental Figure II. *Pulse chase analysis of Apoe$^{4/4}$ and Apoe$^{4/4}$Ldlr$^{h/+}$ hepatocytes*. Cell-associated apoE (synthesis, time 0) during a 60 min pulse and after a 4hr chase (retention) and apoE in medium (secretion) was immunoprecipitated and separated by SDS-PAGE. ^{35}S-Methionine in each band was measured using phosphoimager. Values shown are average of three wells. The experiment was repeated with a similar result. ** $p \leq 0.005$

Supplemental Figure III.

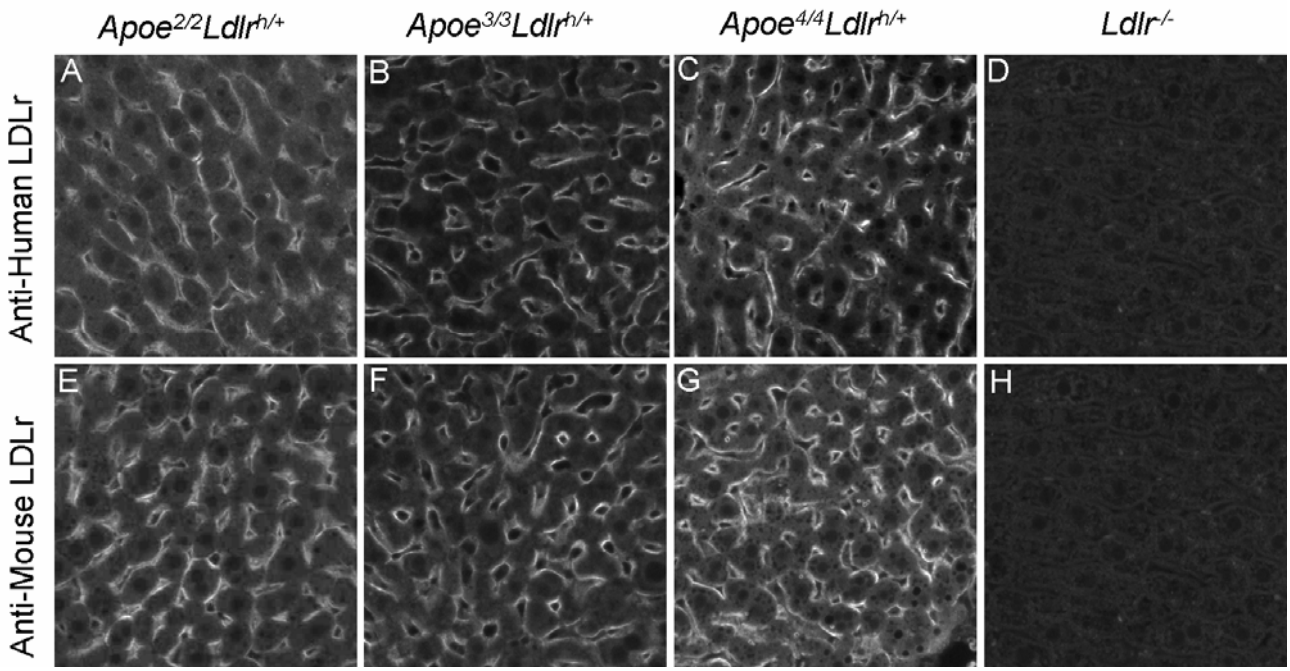

Supplemental Figure III. *Immunohistochemical localization of LDLR in the liver of mice*. Top row, Anti-human LDLR staining of (*A*) *Apoe*$^{2/2}$*Ldlr*$^{h/+}$, (B) *Apoe*$^{3/3}$*Ldlr*$^{h/+}$, (C) *Apoe*$^{4/4}$*Ldlr*$^{h/+}$, and (D) *Apoe*$^{4/4}$*Ldlr*$^{-/-}$ liver. (*A*). Bottom row, staining for anti-mouse LDLR apoE in (E) *Apoe*$^{2/2}$*Ldlr*$^{h/+}$, (F) *Apoe*$^{3/3}$*Ldlr*$^{h/+}$, (G) *Apoe*$^{4/4}$*Ldlr*$^{h/+}$, and (H) *Apoe*$^{4/4}$*Ldlr*$^{-/-}$ livers. (600X).

Supplemental Figure IV.

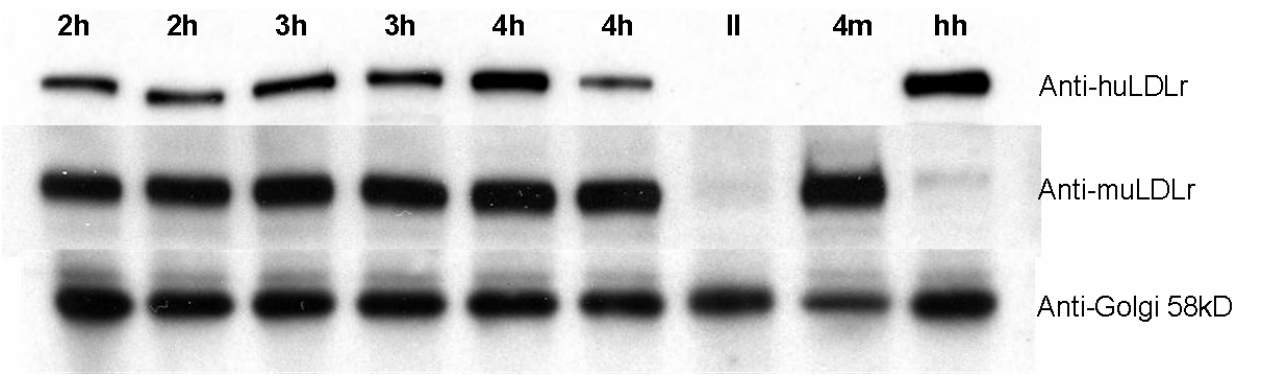

Supplemental Figure IV. *Liver membrane LDLR levels*. Western blots using antibodies specific for the human LDLR (top) and mouse LDLR (middle). 10 µg protein of liver sample was loaded in each lane subjected to SDSPAGE. An antibody to the membrane protein Golgi 58 KdA was used as a loading control (bottom). The 3 lanes furthest to the right (ll, 4m, hh) indicate the minimal cross-reactivity between anti-huLDLR with muLDLR, and anti-MuLDLR and huLDLR.

Supplemental Figure V.

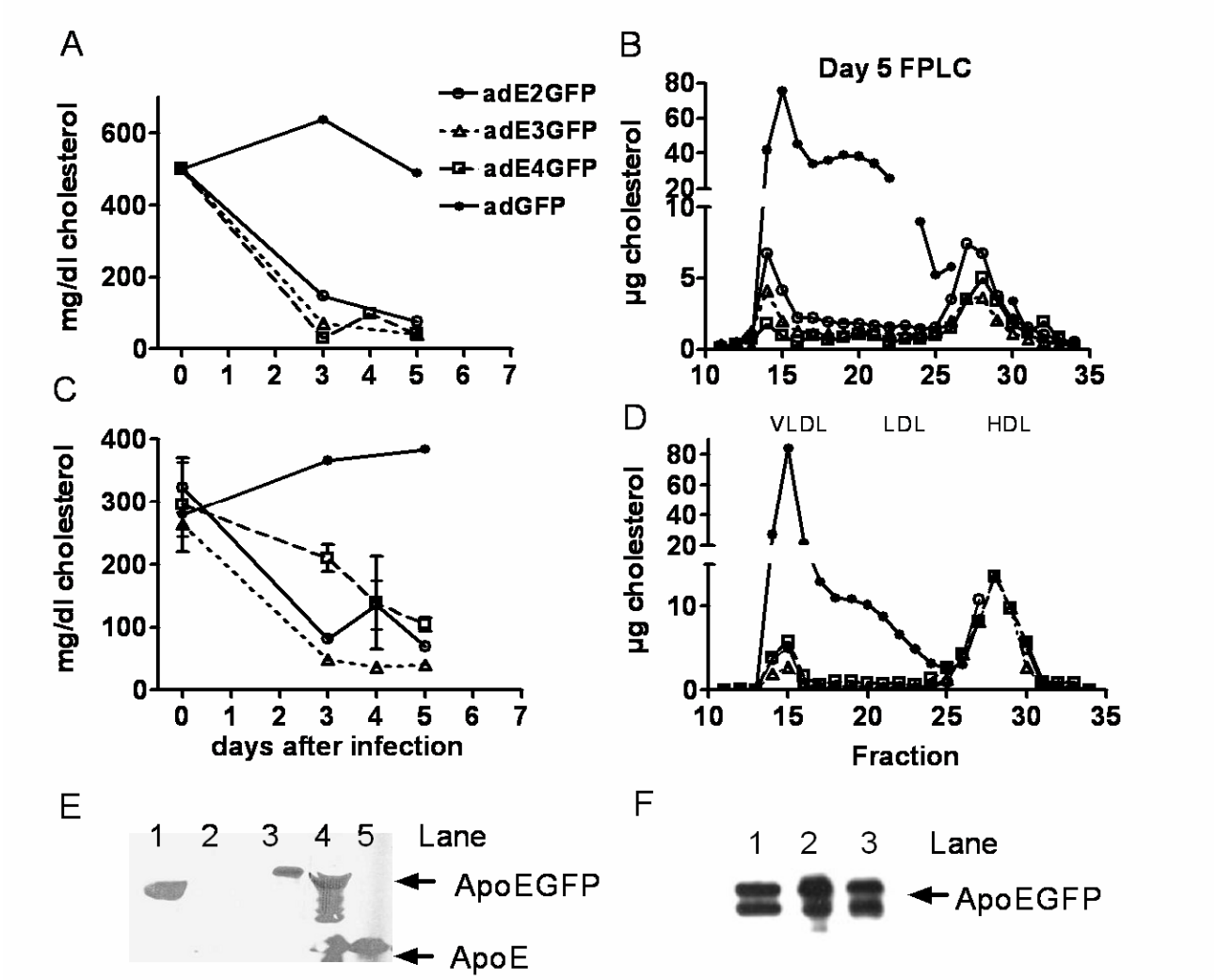

Supplemental Figure V. *Effect of Ad-apoE-GFP on plasma lipid levels.* Plasma cholesterol levels were monitored over 5 days in (*A*) the *Apoe*$^{-/-}$ mice and *(C)* the *Apoe*$^{-/-}$*Ldlr*$^{h/h}$ mice transfected with Ad-apoE2-GFP (black circles with solid line), Ad-apoE3-GFP (open triangles with dotted line), Ad-apoE4-GFP (black squares with dashed line), or Ad-GFP (black dots with solid line). Distribution of cholesterol among different lipoprotein fractions was assessed by FPLC of plasma samples at day 5 in (*B*) the *Apoe*$^{-/-}$ mice and (*D*) the *Apoe*$^{-/-}$*Ldlr*$^{h/h}$ mice. (*E)*, Western blot of plasma from *Apoe*$^{-/-}$ mice transfected with Ad-apoE3-GFP (*lane 1*) or without transfection (*lane 2*), VLDL isolated from Ad-apoE3-GFP transfected *Apoe*$^{-/-}$ mice (*lane 3*), plasma of wild type C57BL/6J mice transfected with Ad-apoE3-GFP (*lane 4*) or without transfection (*lane 5*). (*F)*, ApoE3-GFP associated with VLDL, LDL, and HDL separated by FPLC (fractions 15, 23 and 28, respectively, in panel *B*) from the *Apoe*$^{-/-}$ mice transfected with Ad-apoE3-GFP. These data demonstrate that apoE-GFP fusion proteins are functional and appear to retain isoform-specific characteristics. Since apoE4-GFP can lower cholesterol when over-expressed by adenoviral vector in the liver of *Apoe*$^{4/4}$*Ldlr*$^{h/h}$ mice, adverse effects of LDLR on plasma lipids must be dependent on the relative ratios between apoE4 and LDLR.

Supplemental Figure VI.

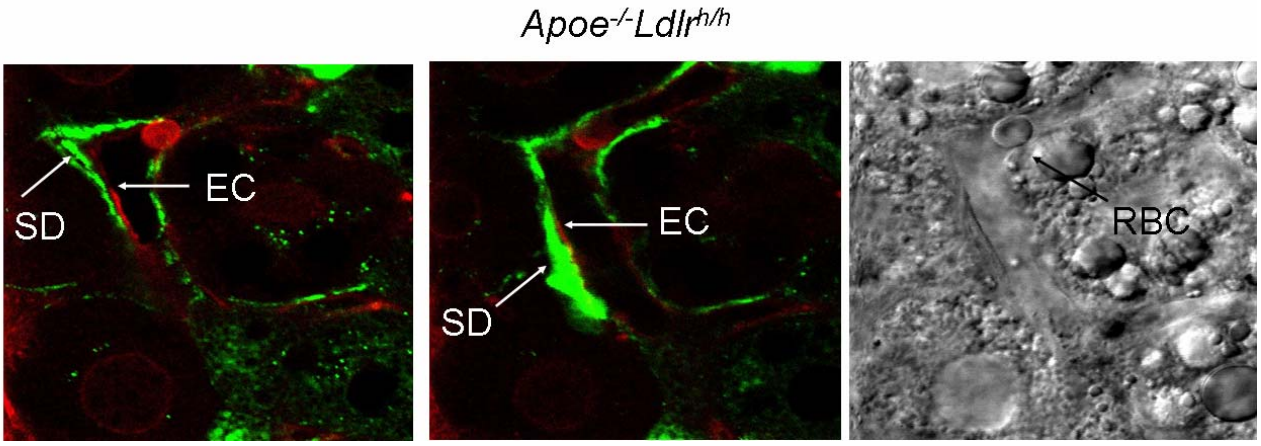

Supplemental Figure VI. *Localization of apoE4-GFP protein on the surface of hepatocytes*. Examination under a higher magnification (1500x) of the two consecutive images shows that apoE4-GFP in the sinusoidal space (SD) in the AdapoE4-GFP transfected *Apoe*$^{-/-}$*Ldlr*$^{h/h}$ liver (green) is localized beneath the endothelial cell lining (EC) stained for lectin (red). Black arrow in the bright field indicates a red blood cell (RBC), which also stained red.

Supplemental Figure VII.

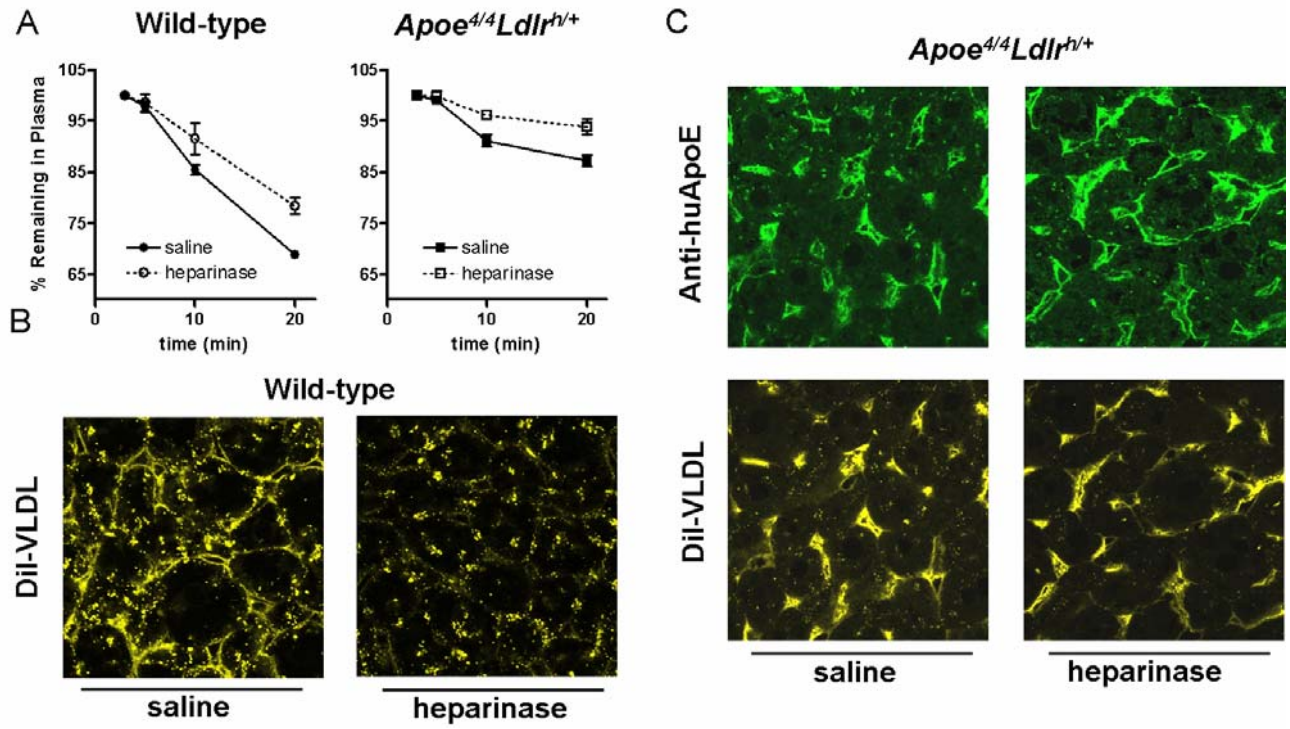

Supplemental Figure VII. *Heparinase effects on VLDL uptake by the liver*. Heparinase (30U/mouse) injected 5 min prior to subsequent injection of apoE$^{-/-}$ DiI labeled VLDL. (A) Clearance of VLDL in wildtype mice (left) and in *Apoe*$^{4/4}$*Ldlr*$^{h/+}$ mice plasma DiI-fluorescence at 2min was taken to be 100%. Both genotypes had a delay in VLDL clearance after heparinase. (B) DiI-fluorescence in wildtype liver 20 min after VLDL injection with saline (left) or heparinase (right). (C) Top panel, apoE immunostaining in 50 µm vibratome sections of *Apoe*$^{4/4}$*Ldlr*$^{h/+}$ liver 20 min after VLDL injection with saline (left) or heparinase (right). (C) Bottom panel, DiI-fluorescence in *Apoe*$^{4/4}$*Ldlr*$^{h/+}$ liver after saline (left) or heparinase (right).

Supplemental Figure VIII

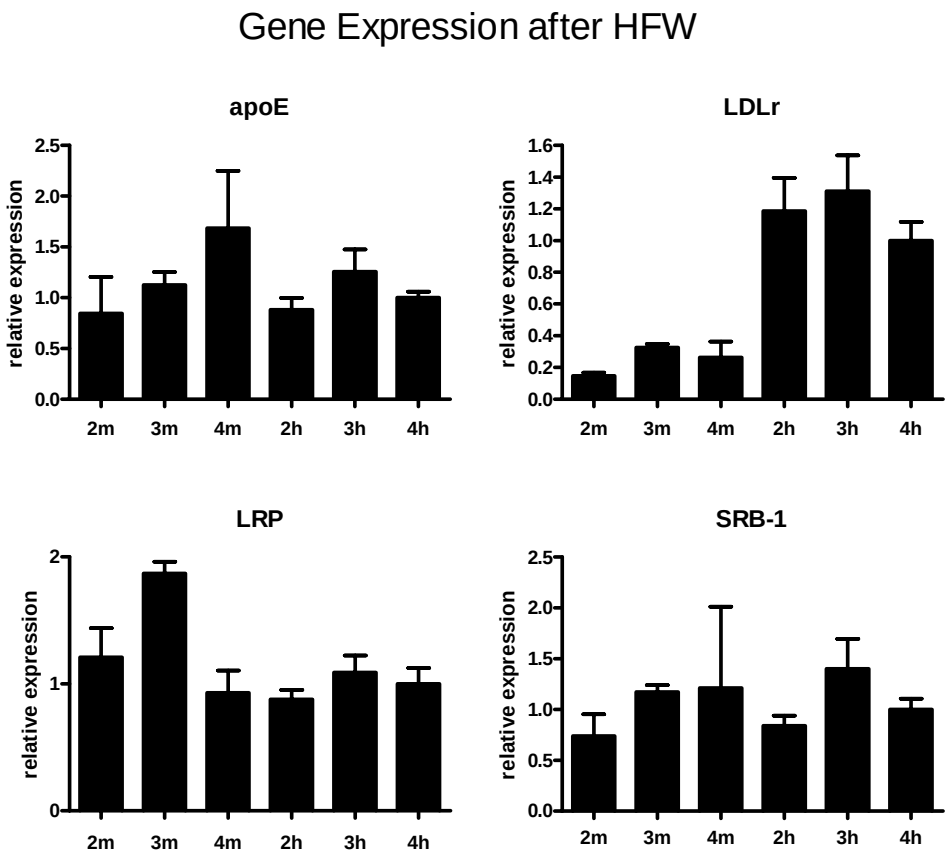

Supplemental Figure VIII. *Gene Expression in the liver*. Relative mRNA levels of the genes were normalized by the expression of β-actin. Values are mean ± S.E. and relative to 4h, which was adjusted to 1. Expressions of apoE, LRP, and SRB-1 were not significantly different among mice with different apoE isoforms. There was an expected increase in LDLR in mice that had the *ldlr*h* allele compared to mice with wildtype *ldlr*. Thus, the effect of apoE isoform on VLDL uptake does not appear to involve pathways affecting expression of apoE, LDLR, LRP, and SRB-1.N > 4 for each genotype.

Supplemental Figure IX.

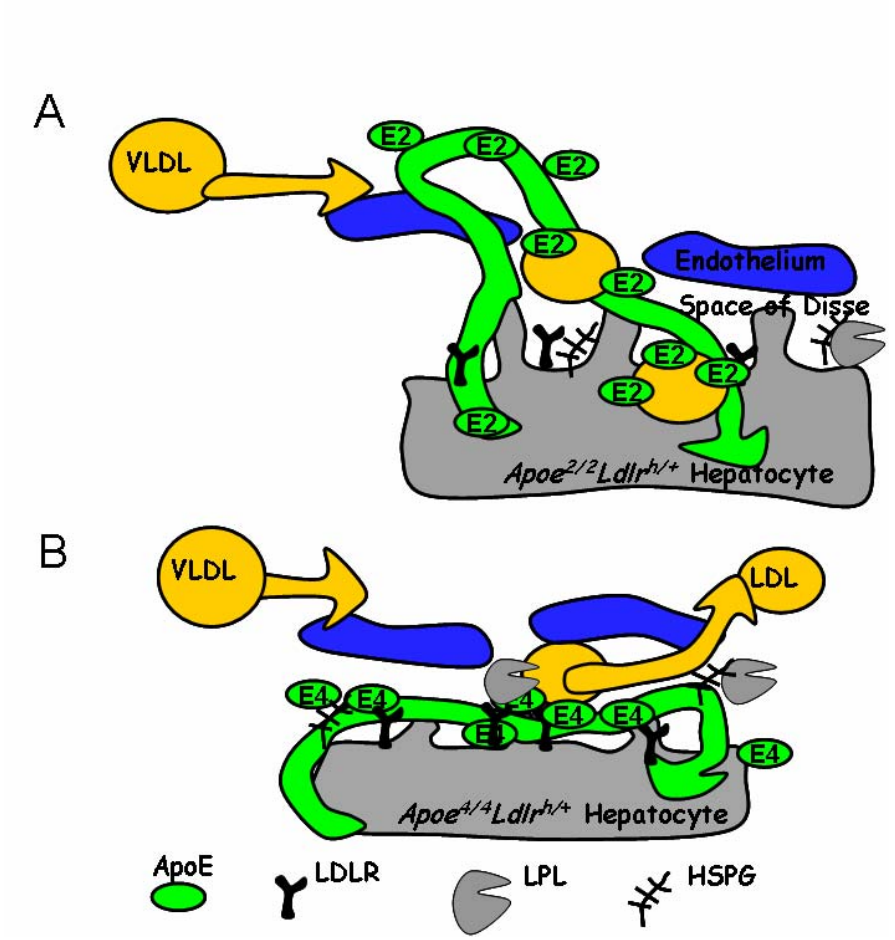

Supplemental Figure IX. *Hypothetical mechanism to explain the potential role of the apoE LDLR interaction on VLDL metabolism*. Endothelial cells (blue) separate the hepatic sinusoid and plasma space from the space of Disse and hepatocyte microvilli (grey). (A) Top diagram shows apoE2 metabolism of apoE-poor VLDL. VLDL (yellow) that has yet to be enriched in apoE enters on the left. The lower LDLR affinity of apoE2 increases the circulation of plasma apoE level (green arrow), and apoE2 locates out of the space of Disse into the plasma. The elevated plasma apoE2 transfers onto VLDL (perhaps from other lipoproteins such as HDL, which is elevated in mice with apoE2). This increases the enrichment of apoE2 onto VLDL which then facilitates LDLR and HSPG mediated uptake without sequestration. (B). Lower diagram shows apoE4 metabolism of apoE-poor VLDL. The life cycle of apoE4 compared to apoE2 is more confined to the space of Disse (green arrow). High LDLR affinity of apoE4 keeps it bound to the hepatic surface, and plasma apoE4 levels are low. ApoE poor VLDL is not enriched with apoE in the plasma as is apoE2. These un-enriched apoE VLDL are stuck at the hepatic surface and are not internalized. The sequestering of VLDL on the surface exposes it to lipases and subsequently they are converted to remnants and LDL.

References

1. Arbones-Mainar JM, Navarro MA, Acin S, Guzman MA, Arnal C, Surra JC, Carnicer R, Roche HM, Osada J. Trans-10, cis-12- and cis-9, trans-11-conjugated linoleic acid isomers selectively modify HDL-apolipoprotein composition in apolipoprotein E knockout mice. *J Nutr.* 2006;136:353-359.
2. Dekroon RM, Armati PJ. Endocytosis of apoE-EGFP by primary human brain cultures. *Cell Biol Int.* 2002;26:761-770.
3. Knouff C, Briand O, Lestavel S, Clavey V, Altenburg M, Maeda N. Defective VLDL metabolism and severe atherosclerosis in mice expressing human apolipoprotein E isoforms but lacking the LDL receptor. *Biochim Biophys Acta.* 2004;1684:8-17.
4. Stephan ZF, Yurachek EC. Rapid fluorometric assay of LDL receptor activity by DiI-labeled LDL. *J Lipid Res.* 1993;34:325-330.
5. Lorenz JN, Gruenstein E. A simple, nonradioactive method for evaluating single-nephron filtration rate using FITC-inulin. *Am J Physiol.* 1999;276:F172-177.
6. Altenburg MK, Johnson LA, Wilder JC, Maeda N. Apolipoprotein E4 in macrophages enhances atherogenesis in an LDL receptor dependent manner. *J Biol Chem.* 2007.